Research Square

Preprints are preliminary reports that have not undergone peer review.
They should not be considered conclusive, used to inform clinical practice,
or referenced by the media as validated information.

Developmental perturbation of Purkinje cell function induces male-biased core and associated autism spectrum disorder–like phenotypes in adulthood

Hideki Miwa

miwahid@iwate-med.ac.jp

Iwate Medical University https://orcid.org/0000-0001-6015-3007

Satoshi Kamijo

Kei Hori

Mikio Hoshino

National Center of Neurology and Psychiatry, NCNP https://orcid.org/0000-0002-9526-3473

Kazutaka Ikeda

Tokyo Metropolitan Institute of Medical Science https://orcid.org/0000-0001-8342-0278

Article

Keywords: Autism, cerebellum, developmental activity, sex-difference, Purkinje cell

Posted Date: November 4th, 2026

DOI: https://doi.org/10.21203/rs.3.rs-11596035/v1

License: This work is licensed under a Creative Commons Attribution 4.0 International License.
Read Full License

Additional Declarations: The authors have declared there is **NO** conflict of interest to disclose

Developmental perturbation of Purkinje cell function induces male-biased core and associated autism spectrum disorder–like phenotypes in adulthood

Running title: Male-biased autism traits via cerebellar deficits

Satoshi Kamijo[1,2], Kei Hori[3], Mikio Hoshino[3], Kazutaka Ikeda[1,4], Hideki Miwa[1,5]*

[1]Department of Neuropsychopharmacology, National Institute of Mental Health, National Center of Neurology and Psychiatry, Kodaira, Tokyo 187-8553, Japan

[2]Department of Physiology, National Medical Defense College, Tokorozawa, Saitama 359-8513, Japan

[3]Department of Biochemistry and Cellular Biology, National Institute of Neuroscience, National Center of Neurology and Psychiatry, Kodaira, Tokyo 187-8502, Japan

[4]Addictive Substance Project, Tokyo Metropolitan Institute of Medical Science, Setagaya, Tokyo 156-8506, Japan.

[5]Division of Bioregulatory Pharmacology, Department of Pharmacology, Iwate Medical

University, Yahaba, Iwate 028-3694, Japan

*Corresponding author

Department of Neuropsychopharmacology, National Institute of Mental Health, National Center of Neurology and Psychiatry, Tokyo 187-8553, Japan; Division of Bioregulatory Pharmacology, Department of Pharmacology, Iwate Medical University, Yahaba, Iwate 028-3694, Japan

E-mail: Hideki_Miwa@ncnp.go.jp or miwahid@iwate-med.ac.jp (H.M.)

Number of figures: 6

Number of tables: 1

Number of supplemental figures: 9

Number of supplemental tables: 1

Key Words: Autism, cerebellum, developmental activity, sex-difference, Purkinje cell

Abstract: 216 words

Introduction: *550* words

Article: 4696 words,

excluding abstract and references.

Abstract

Autism spectrum disorder (ASD) is a prevalent neurodevelopmental condition whose etiology remains incompletely understood. Human epidemiological studies have implicated the cerebellum in ASD pathogenesis, and studies in mouse models have provided evidence for a causal contribution of cerebellar dysfunction. However, previous animal studies have largely focused on males and cerebellar manipulations at later developmental stages, with associated features of ASD remaining less explored. To address these gaps, we chemogenetically perturbed Purkinje cell function during early postnatal development in both male and female mice. Developmental Purkinje cell perturbation induced male-biased core ASD-like behavioral phenotypes, including reduced sociability and cognitive inflexibility. Phenotypes related to associated features of ASD, including impaired fine motor learning, altered sensory processing, and sleep abnormalities, were also predominantly observed in males. At the molecular level, bulk RNA sequencing following developmental

Purkinje cell perturbation identified candidate sex-dependent transcriptional changes in both the hindbrain and forebrain, suggesting that altered cerebellar activity during development can influence gene expression across distant brain regions. Together, these findings demonstrate that transient early postnatal perturbation of Purkinje cell function can produce diverse core and associated ASD-like phenotypes, predominantly in males, with evidence suggesting transcriptional changes beyond the cerebellum. This study highlights developmental cerebellar dysfunction as a potential contributor to sex differences in ASD vulnerability.

Introduction

Autism spectrum disorder (ASD) is a common neurodevelopmental condition affecting approximately 2-3% of the population in developed countries (1-4), with substantially higher diagnosed prevalence in males than in females (5). Complex interactions between genetic and environmental factors contribute to ASD, and multiple mechanisms, including synaptic dysfunction (6), altered neuroimmune modulation (7), serotonergic dysfunction (8), and epigenetic dysregulation (9), have been implicated. Nevertheless, the neural mechanisms through which these diverse etiological factors give rise to ASD remain incompletely understood (10-12).

Accumulating evidence has identified the cerebellum as a critical node in the pathogenesis of ASD (13, 14). Beyond its well-established role in motor control, the cerebellum contributes to higher-order cognitive and affective processing, and cerebellar lesions are associated with persistent behavioral abnormalities (15, 16). Human epidemiological studies show that perinatal cerebellar injury markedly increases the risk of developing ASD by up to 36-fold (17), and postmortem studies consistently reveal reduced Purkinje cell numbers in individuals with ASD (18). Reductions in cerebellar gray matter have also been associated with the severity of core ASD symptoms (19). Although ASD is

77 highly heterogeneous, these converging findings suggest that cerebellar dysfunction may
78 represent a shared pathophysiological feature across etiologically diverse forms of ASD.

79 Studies in rodent models further support a causal contribution of cerebellar
80 dysfunction to ASD-like phenotypes (20-27). Purkinje cell-specific deletion of the *Tsc1* gene
81 induces core ASD-like behaviors (28), and these phenotypes can be partially rescued by
82 correcting the overactivation of mTOR signaling (29). In addition, transient activation of
83 Purkinje cells during the juvenile period (postnatal days 30-56) induces region-specific ASD-
84 like behaviors in adulthood (30), indicating that aberrant Purkinje cell activity during
85 development can have long-lasting behavioral consequences. Together, these studies support
86 a causal role for cerebellar dysfunction in the emergence of ASD-like phenotypes.

87 Despite these advances, several important questions remain. First, previous studies
88 have primarily manipulated Purkinje cell function at relatively late developmental stages,
89 leaving the earlier developmental window implicated by human epidemiological studies
90 largely unexplored. It therefore remains unclear whether transient perturbation of Purkinje
91 cell function during an earlier, perinatal-equivalent window is sufficient to induce ASD-like
92 phenotypes. Second, most studies have focused exclusively on male animals, and whether
93 developmental cerebellar dysfunction differentially affects males and females remains

largely unknown. Finally, previous studies have rarely evaluated features commonly associated with ASD (31), including sensory hypersensitivity or hyposensitivity, sensory gating deficits, fine motor impairments, and sleep dysregulation. Thus, whether developmental cerebellar dysfunction can induce both core ASD-like behaviors and a broader range of associated phenotypes remains unresolved.

To address these questions, we examined whether transient perturbation of Purkinje cell function during a perinatal-equivalent window induces ASD-like phenotypes in a sex-dependent manner. We chemogenetically perturbed Purkinje cell function and assessed core ASD-like traits together with motor, sensory, and sleep-related phenotypes in both male and female mice. Developmental Purkinje cell perturbation produced multiple behavioral abnormalities, including reduced social preference and cognitive inflexibility, with a pronounced male bias, as well as several phenotypes related to associated features of ASD. Bulk RNA sequencing further identified candidate sex-dependent transcriptional changes in both the hindbrain and forebrain following Purkinje cell perturbation. Together, these findings demonstrate that transient developmental Purkinje cell dysfunction can produce a broad spectrum of ASD-like phenotypes and suggest greater vulnerability to developmental cerebellar perturbation in males.

Materials and Methods

A detailed description of the Materials and Methods is provided in the Supplementary Information.

Animals

L7-Cre mice (32) were crossed with LSL-hM4Di-DREADD-mCitrine mice (33) to generate Cre-positive and Cre-negative littermates. Wild-type C57BL/6J mice were obtained from Japan SLC (Shizuoka, Japan). Both male and female mice were used. Animals were maintained under a 12-h light/dark cycle with food and water available ad libitum. All procedures were approved by the National Center of Neurology and Psychiatry.

Genotyping

Genotypes were determined by PCR and, in more than 80% of animals, further confirmed histologically by Cre-dependent hM4Di-mCitrine expression in Purkinje cells. Primer sequences are provided in Supplementary Table 1.

Developmental chemogenetic perturbation of Purkinje cells

Clozapine-N-oxide dihydrochloride (CNO, 5 mg/kg; Hello Bio, Bristol, UK) was

129 administered orally once daily to Cre-positive and Cre-negative littermates during P11-15,
130 P11-20, or P21-30, as previously described (34).
131
132 ***In vitro* slice electrophysiology**
133 Whole-cell patch-clamp recordings were performed in large glutamatergic neurons of the
134 deep cerebellar nuclei in acute cerebellar slices from P15–20 naïve L7-Cre; hM4Di mice, as
135 previously described (35). Inhibitory postsynaptic currents were evoked by electrical
136 stimulation of Purkinje cell axons and recorded at 0 mV before and during CNO application.
137 Paired-pulse responses were measured using a 100-ms interstimulus interval, and the paired-
138 pulse ratio and $1/CV^2$ were used to assess presynaptic effects.
139
140 **Behavioral analyses**
141 Behavioral testing began at 8 weeks of age and was performed largely as previously described
142 (35). The behavioral battery comprised open field, marble burying, three-chamber social
143 interaction, accelerating rotarod, grooming, elevated plus maze, acoustic startle response
144 (ASR)/prepulse inhibition (PPI), and Barnes maze tests. Locomotor activity was assessed in
145 the open field, repetitive behavior by marble burying and grooming, motor coordination by

the accelerating rotarod, and anxiety-like behavior in the elevated plus maze. In the three-chamber test, investigation of social and object stimuli was measured, and social preference was calculated as

$$Social\ preference\ index\ = \frac{time_{social} - time_{object}}{time_{social} + time_{object}}$$

For ASR, startle responses to 70–120 dB stimuli were measured. For PPI, prepulses of 0, 70, 75, or 80 dB preceded a 120 dB startle stimulus by 100 ms. PPI was calculated as

$$\text{PPI (\%)} = 100 \times \left[1 - \frac{\text{ASR amplitude in startle with prepulse trials}}{\text{ASR amplitude in startle alone trials}}\right]$$

Animals whose response to the 120 dB stimulus was less than five times their baseline response during 0 dB trials were excluded from ASR/PPI analyses.

Spatial learning and cognitive flexibility were assessed using the Barnes maze, comprising acquisition (days 1-5), probe (day 6), reversal learning (days 7-9), and reversal probe phases (day 10). Primary latency was defined as the time to first locate the correct goal hole and was

used to assess training performance. The arena was divided into four zones, each containing five holes, with the target hole serving as a reference point. Investigation time was defined as the total time spent investigating the holes within each quadrant. During the reversal probe test, search strategies were classified according to whether mice preferentially explored the old or new target zone in each 60-s segment. Strategy switches were defined as transitions between these two search strategies across consecutive segments. Persistence with the same strategy, despite its failure to guide the animal to the new target location, was interpreted as reduced behavioral flexibility

Electroencephalographic (EEG)/Electromyographic (EMG) recordings and sleep-wake analysis

Adult mice were chronically implanted with cortical EEG and neck EMG electrodes and allowed to recover for at least 2 weeks before recording. Following 2 days of habituation, continuous EEG/EMG signals were recorded and vigilance states were manually classified in 4-s epochs as wakefulness, non-rapid-eye-movement (NREM) sleep, or rapid-eye-movement (REM) sleep, as previously described (36). Total time, bout number, and mean bout duration were quantified for each vigilance state, together with EEG power spectral

density.

Histology

Mice were transcardially perfused with 4% paraformaldehyde/phosphate buffer, and brains were sagittally sectioned at 50 μm. Cerebellar sections were immunostained for mCitrine and calbindin to assess Cre-dependent mCitrine expression in Purkinje cells. Fluorescence and confocal microscopy were used for imaging. Antibody information and detailed procedures are provided in the Supplementary Information.

Transcriptomic analyses

For transcriptomic analysis, CNO (5 mg/kg) was administered once daily from P11 to P15, and the forebrain and hindbrain were collected 4 h after the final dose. Total RNA was extracted and treated with DNase before analysis. RNA sequencing was performed using three biological replicates per sex and genotype for each brain region. For exploratory identification of transcriptional changes, genes with $|\log_2 \text{fold change}| > \log_2(1.25)$, unadjusted $P < 0.01$, and $\log_2(\text{counts per million}) > 4$ were selected. Expression of *Gabra2*, *Pop4* and mCitrine was examined by quantitative RT-PCR using *Ywhaz* as the reference gene

and the ΔΔCt method. Primer sequences are provided in Supplementary Table 1.

Statistical analyses

Data are presented as mean ± SEM. Statistical comparisons were performed using two-tailed unpaired *t*-tests or two-way repeated-measures ANOVA, unless otherwise specified. Sample sizes and additional statistical details are provided in the figure legends. Analyses were performed using GraphPad Prism 10, with $P < 0.05$ considered statistically significant.

Results

Establishing a temporally controlled Purkinje cell inhibition paradigm during early postnatal development

To achieve temporally controlled and reversible inhibition of Purkinje cells (PCs) during development, we employed the designer receptors exclusively activated by designer drugs (DREADD) system (Fig. 1A, top) (37). Heterozygous L7-Cre mice, which express Cre recombinase specifically in most PCs (32), were crossed with homozygous LSL-hM4Di-mCitrine mice, enabling Cre-dependent expression of the inhibitory DREADD hM4Di (33). This breeding strategy yielded Cre-positive offspring expressing hM4Di and the fluorescent protein mCitrine in PCs, and Cre-negative littermates serving as controls.

To examine the effects of PC inhibition across developmental stages, we administered clozapine-N-oxide (CNO) orally to pups of both genotypes. Because the human perinatal period approximately corresponds to the second postnatal week in mice (38-40), we defined three inhibition periods: P11–15 (postnatal days 11-15), P11–20, and P21–30 (Fig. 1A, bottom), all of which began earlier than the intervention used in a previous study (34). Cre-positive mice expressing hM4Di in Purkinje cells are hereafter referred to as PC-inhibited mice, and their Cre-negative counterparts as controls.

We first confirmed PC-specific, Cre-dependent hM4Di expression by mCitrine fluorescence at P16 (Fig. 1B). mCitrine expression was detectable by P10, one day before the earliest intervention time point (Supplementary Fig. 1A). Consistent with previous reports (33), Cre-independent mCitrine signals were also observed in the hippocampal dentate gyrus, olfactory bulbs, and retrosplenial cortex (Supplementary Figs. 1B-C). Nevertheless, robust Cre-dependent hM4Di expression was restricted to Purkinje cells in the cerebellum (Supplementary Figs. 1B-C). RT-qPCR further demonstrated increased mCitrine expression in the hindbrain of Cre-positive mice, consistent with the histological findings (Supplementary Fig. 1D).

We next verified the functional efficacy of hM4Di-mediated PC inhibition using acute cerebellar slices (Fig. 1C, top). Because PCs provide inhibitory inputs to neurons in the deep cerebellar nuclei (DCN), we recorded evoked inhibitory postsynaptic currents (IPSCs) from DCN neurons in acute cerebellar slices prepared from naïve Cre-positive hM4Di-expressing mice (P15–P20) by stimulation of Purkinje cell axons (Fig. 1C, bottom). Bath application of CNO significantly reduced IPSC amplitudes (Fig. 1D). CNO also increased the paired-pulse ratio (Fig. 1E), supporting a reduction in presynaptic release probability.

Analysis of the inverse squared coefficient of variation ($1/CV^2$) of IPSC amplitudes further supported a presynaptic mechanism (data not shown). These results confirmed that activation of hM4Di reduced inhibitory transmission from PCs to DCN neurons.

Finally, we examined whether developmental PC inhibition produced lasting effects on PC survival or cerebellar cytoarchitecture. Linear PC density in lobule IX of adult mice was comparable between PC-inhibited and control groups across all three intervention periods (Fig. 1F), and no overt cytoarchitectural abnormalities were observed (data not shown). Because the cerebellum plays a major role in motor control, we also assessed locomotor performance in the open field test (Supplementary Fig. 1E). Although males subjected to P11–15 inhibition exhibited a slight reduction in locomotion speed, no significant differences were detected under the other conditions. Together, these results establish a temporally controlled developmental PC inhibition paradigm that reduces PC output without detectable long-term loss of PCs or overt disruption of cerebellar architecture. We therefore proceeded to behavioral analyses.

Transient developmental PC perturbation induced male-biased alterations in core ASD-like behaviors.

Reduced sociability is a core behavioral feature of ASD. We conducted a three-chamber social interaction test to assess whether developmental PC inhibition affects sociability (41, 42). Males subjected to P11–15 PC inhibition exhibited a moderate reduction in social preference (Fig. 2A, left). Although males subjected to P11–20 and P21–30 PC inhibition also showed lower median social preference, these differences did not reach statistical significance. The reduced social preference in P11–15 males was driven by increased object investigation, rather than decreased social investigation (Supplementary Figs. 2A, B). In contrast, PC-inhibited females displayed social preference comparable to controls across all intervention periods (Fig. 2A, right).

Next, we assessed repetitive behavior using a grooming test. Developmental PC inhibition did not alter total grooming duration in any group (Fig. 2B). Although P21–30 PC-inhibited males showed a trend toward increased grooming, the difference was not statistically significant. The marble burying test likewise revealed no group differences (Supplementary Fig. 3). Thus, repetitive behaviors were not detectably altered in adulthood.

To assess ASD-related cognitive inflexibility, we performed a reversal Barnes maze test (Fig. 3A) (43-45). During the initial learning phase, primary latency did not differ between PC-inhibited and control mice in either sex (Fig. 3B). In the subsequent probe test,

all groups preferentially explored the target area, and target investigation time did not differ between PC-inhibited and control mice (Fig. 3C), indicating intact spatial learning and memory. During reversal learning, primary latency likewise remained comparable between groups (Fig. 3B). In the reversal probe test, all groups preferentially investigated the new target over the original target location (Fig. 3C). However, males subjected to P11–20 PC inhibition exhibited fewer switches between search strategies across consecutive segments (Table 1 and Supplementary Fig. 4), indicating reduced updating of search strategy following unsuccessful attempts, consistent with impaired cognitive flexibility.

In summary, transient developmental PC inhibition induced modest behavioral phenotypes relevant to core ASD symptoms in adulthood, including reduced social preference and altered search strategy during the reversal probe test, predominantly in males, without clear induction of repetitive behaviors. These findings indicate that transient cerebellar dysfunction during development can produce male-biased, alterations in sociability and cognitive flexibility in adulthood, with the observed phenotypes differing across intervention periods.

Developmental PC perturbation induces ASD-associated alterations in motor

coordination and sensorimotor processing in a sex- and timing-dependent manner.

Beyond core ASD-like behaviors, we next asked whether developmental cerebellar dysfunction also contributes to ASD-associated features, including motor coordination difficulties, anxiety, sensory abnormalities, and sleep disturbances (31, 46-49). We assessed motor coordination and motor skill learning using an accelerating rotarod test. Males subjected to P11–15 PC inhibition exhibited a shorter latency to fall than controls (Fig. 4A). Prolonged P11–20 PC inhibition produced a milder effect, whereas delayed P21–30 PC inhibition showed the opposite trend. In contrast, females subjected to P11–15 PC inhibition showed a trend toward longer latency to fall. Thus, the effect of developmental PC inhibition on motor performance differed across intervention periods and between sexes.

We next evaluated anxiety-like behavior using the elevated-plus maze. Time spent in the open arms did not differ between PC-inhibited and control mice in either sex (Supplementary Fig. 5), indicating no detectable alterations in anxiety-like behavior in adulthood.

To assess auditory sensorimotor processing, we measured acoustic startle response (ASR) and prepulse inhibition (PPI). Although group differences in ASR did not reach statistical significance, startle amplitudes tended to be reduced in males following P11–15

307 inhibition and in females following P11–20 inhibition, whereas males subjected to P21–30
308 inhibition showed the opposite trend (Fig. 4B; Supplementary Fig. 6). We next evaluated PPI
309 as an index of sensorimotor gating (Fig. 4C). Although alterations in PPI have been reported
310 in ASD, findings have been inconsistent (50). In males, PPI was significantly reduced
311 following P11–20 PC inhibition, whereas P21–30 inhibition produced a similar trend that did
312 not reach statistical significance. In females, P11–20 PC inhibition significantly increased
313 PPI, while P11–15 inhibition showed the opposite trend. Together, these findings indicate
314 that developmental PC inhibition alters auditory sensorimotor processing in a manner that
315 varies with developmental timing and sex.
316
317 **Developmental perturbation of Purkinje cell function alters sleep–wake architecture in**
318 **male mice.**
319 Sleep disturbances are common in individuals with ASD and have been associated with the
320 severity of behavioral symptoms (49, 51). We therefore recorded electroencephalograms
321 (EEGs) from adult male and female mice subjected to P11–20 PC inhibition and their
322 respective controls to determine whether developmental perturbation of Purkinje cell
323 function alters sleep–wake architecture in adulthood. Representative 24-h hypnograms are

shown in Fig. 5A. Analysis of the 24-h time course revealed significant group effects on wakefulness, NREM sleep, and REM sleep (Fig. 5B). Across the entire 24-h period, male PC-inhibited mice spent significantly less time awake and more time in NREM sleep than male controls, whereas no significant differences were observed in females (Fig. 5C). These differences were most prominent during the dark phase. Male PC-inhibited mice spent significantly less time awake and more time in NREM sleep than male controls, whereas no significant differences were detected during the light phase or in females during either phase (Fig. 5D). We therefore examined sleep–wake architecture in greater detail during the dark phase, while the corresponding light-phase analyses are shown in Supplementary Fig. 7.

During the dark phase, male PC-inhibited mice showed a numerical increase in the number of wake episodes and a shorter mean wake episode duration, although these differences did not reach statistical significance (Fig. 5E). REM episode numbers also tended to be increased, whereas mean REM episode duration was unchanged. Analysis of episode-duration distributions revealed an increased number of short wake episodes and a markedly reduced contribution of very long (>4096 s) wake episodes to total wake time (Fig. 5F). For NREM sleep, intermediate-duration episodes contributed more to total NREM sleep time. REM sleep likewise showed an increased number of short-to-intermediate-duration episodes,

and a corresponding increase in their contribution to total REM sleep time. Wake-to-NREM transitions were significantly increased in male PC-inhibited mice, whereas other vigilance-state transitions were not significantly altered (Fig. 5G). During the light phase, although overall vigilance-state durations were unchanged, male PC-inhibited mice similarly showed a reduced contribution of long-duration wake episodes to total wake time (Supplementary Fig. 7).

Finally, we examined EEG spectral characteristics during each vigilance state. EEG power spectra during the dark phase were comparable between groups (Fig. 5H), with no significant differences in total power or relative delta, theta, sigma, or beta power (Supplementary Fig. 8). During the light phase, male PC-inhibited mice showed reduced relative delta power during REM sleep (Supplementary Fig. 7).

Together, these findings indicate that developmental perturbation of Purkinje cell function produces alterations in sleep–wake regulation in adult male mice, characterized particularly by reduced maintenance of sustained wakefulness and increased sleep during the dark phase.

Developmental PC perturbation induced transcriptional changes in the hindbrain and

forebrain with sex-dependent patterns.

To determine whether transient developmental PC perturbation also produces sex-dependent molecular alterations, we performed RNA sequencing on hindbrain and forebrain tissue collected at P15 from male and female mice subjected to P11–15 PC inhibition and their respective controls (Fig. 6A). Sex-stratified analysis identified candidate transcriptional changes in both brain regions (Supplementary Fig. 9). Multiple candidate differentially expressed genes (DEGs) were detected in the hindbrain and forebrain, suggesting that developmental PC perturbation affects gene expression beyond the cerebellum. As representative examples, we selected two candidate DEGs identified in males, *Gabra2* and *Pop4*, for validation by RT-qPCR. The RT-qPCR results showed a similar pattern of increased expression in males (Fig. 6B). Together, these findings suggest that five days of Purkinje cell perturbation during early postnatal development can induce transcriptional changes not only in the hindbrain but also in the forebrain, with patterns that differ between males and females.

Discussion

ASD is a neurodevelopmental disorder characterized by marked clinical heterogeneity and a pronounced male bias in diagnosis (1-4). Previous rodent studies, including developmental

perturbation of cerebellar circuits, have established that altered cerebellar activity during development can produce persistent ASD-like behavioral phenotypes (20-30). Our findings extend this work by showing that transient perturbation of Purkinje cell function during an earlier postnatal, human perinatal-equivalent developmental window produces modest but ASD-relevant behavioral alterations in adulthood with a pronounced male bias. The effects extended beyond core ASD-like behaviors to motor, sensory, and sleep-related phenotypes and were accompanied by candidate transcriptional changes in both the hindbrain and forebrain. Together, these findings broaden the proposed role of developmental cerebellar dysfunction in ASD by highlighting sex-biased vulnerability, associated behavioral features, and long-range molecular consequences.

A major finding of our study is the male-biased behavioral susceptibility to developmental PC perturbation. Core ASD-relevant phenotypes were more consistently affected in males: social preference was reduced following P11–15 inhibition, and cognitive flexibility was impaired following P11–20 inhibition, whereas females showed no detectable changes in these domains. Associated phenotypes also showed prominent sex differences. Fine motor performance was impaired in males following P11–15 inhibition, and PPI was reduced in males but increased in females following P11–20 inhibition. Sleep–wake

abnormalities were likewise detected predominantly in males. Thus, although the specific effects varied across behavioral domains and intervention periods, males showed greater overall susceptibility to transient developmental PC dysfunction.

This pattern mirrors the well-established male bias in ASD. Motor coordination difficulties are frequently reported in individuals with ASD, with many meeting diagnostic criteria for developmental coordination disorder (DCD) (46), which itself shows a male predominance (52) . Sleep disturbances are also highly prevalent in ASD (49, 51, 53, 54). In the present study, developmental PC perturbation altered sleep–wake organization in adult males, particularly by reducing sustained wakefulness during the active phase. Although the direction of individual sleep-stage changes does not necessarily correspond to those reported in individuals with ASD, impaired sleep–wake organization may recapitulate an important associated feature of the disorder. Together, these findings raise the possibility that male-biased vulnerability of the developing cerebellum may extend across neural systems contributing to both core and associated ASD-relevant features.

Several developmental mechanisms could contribute to this male-biased susceptibility. Purkinje cells undergo electrophysiological maturation approximately four days earlier in males than in females (55), potentially creating sex-dependent differences in

409 vulnerability during early postnatal development. GABAergic signaling also undergoes
410 substantial developmental changes during this period. In the cerebellum, the developmental
411 polarity shift in GABAergic signaling occurs during the second and third postnatal weeks,
412 overlapping with the intervention periods examined here, and prenatal valproic acid (VPA)
413 exposure delays this shift (55). Additional evidence points to sex differences in the
414 vulnerability of PCs themselves. Male-biased PC loss has been reported in VPA-exposed and
415 *reeler* mice (56-58), whereas female PCs exhibit higher levels of calbindin, which may
416 enhance resistance to calcium-mediated excitotoxicity (59). Estradiol also promotes dendritic
417 development of PCs during the second postnatal week and may contribute to greater
418 resilience in females (60). These observations provide several potential mechanisms for sex-
419 dependent responses to developmental cerebellar perturbation, although their relative
420 contributions remain to be established.

421 Although ASD is highly heterogeneous, diverse genetic and environmental risk
422 factors may converge on cerebellar developmental programs. PC-specific deletion of ASD-
423 relevant genes, including *Th*, *Tsc1*, *Tsc2*, *Pten*, *Mecp2*, *Auts2*, *Shank2*, *Fmr1*, and *Scn8a*, is
424 sufficient to elicit ASD-like phenotypes in mouse models (20-29, 61-63), underscoring the
425 contribution of Purkinje cells to ASD-relevant neurodevelopmental processes. Serotonergic

signaling influences dendritic arborization of developing PCs via 5-HT_3A receptors (64), whereas inflammation suppresses dendritic expansion through prostaglandin E_2-dependent pathways (60). In utero exposure to VPA also reduces PC number in rodents (56, 65). In preterm infants, the cerebellum exhibits increased expression of myelin proteins together with white matter changes consistent with accelerated myelination. These alterations have been linked to insufficient levels of placenta-derived allopregnanolone, a neurosteroid that acutely enhances GABAergic signaling through $GABA_A$ receptors. Intriguingly, these effects appear to be more pronounced in males, suggesting male-biased vulnerability of cerebellar development following preterm birth (66). Thus, genetically and mechanistically diverse ASD risk factors may converge on the development or function of the cerebellum, making developmental cerebellar dysfunction a plausible shared substrate for overlapping ASD-relevant phenotypes.

An additional finding of our study is that the consequences of developmental PC perturbation were not confined to the cerebellum. Bulk RNA sequencing at P15 identified candidate transcriptional changes in both the hindbrain and forebrain, with distinct patterns observed in males and females. Among the candidate changes identified in males, *Gabra2* and *Pop4* were selected as representative genes for RT-qPCR validation, and their upregulation was

443 confirmed. *Gabra2* encodes the α2 subunit of $GABA_A$ receptors and is expressed in
444 cerebellar Golgi cells and excitatory neurons of the deep cerebellar nuclei (67, 68). *Pop4* has
445 been implicated in chromatin-associated processes, including activity-dependent histone
446 H3.3 exchange (69, 70). The broader implication of these transcriptomic findings is that
447 transient developmental cerebellar perturbation can be accompanied by molecular changes
448 in anatomically distant brain regions. This remote effect may represent a developmental
449 diaschisis-like process, whereby altered cerebellar activity influences function or gene
450 expression in connected forebrain circuits.

451 The phenotypes elicited by developmental PC inhibition in our study were milder
452 than those reported in previous animal models (28-30). Several factors may account for this
453 difference. First, the extent of PC dysfunction induced by our manipulation may have been
454 relatively limited. Unlike the permanent genetic deletions or sustained perturbations used in
455 previous studies, our PC inhibition was brief (5–10 days) and intermittent. Moreover, our
456 electrophysiological data showed that CNO reduced, but did not abolish, PC-mediated
457 inhibitory transmission. Second, developmental compensation may have attenuated
458 behavioral phenotypes. Because our experimental design cannot distinguish compensated
459 animals from those that were intrinsically unaffected, the phenotypes that remained

460 detectable in adulthood may represent behavioral domains that were relatively resistant to
461 compensation. Third, the developmental processes affected by PC inhibition likely differed
462 among intervention periods and behavioral domains. Finally, the absence of certain ASD-
463 relevant phenotypes may reflect differences in the extent to which individual behavioral
464 domains depend on cerebellar function.

465 The variable effects observed across intervention periods also merit consideration.
466 We initially expected that the longer P11–20 inhibition would produce more pronounced
467 effects than the shorter P11–15 inhibition. Instead, a simple relationship between intervention
468 duration and behavioral severity was not evident. Social preference was most clearly affected
469 following P11–15 inhibition, whereas cognitive flexibility was altered following P11–20
470 inhibition, and motor effects also differed across intervention periods. Because the first
471 postnatal month encompasses rapid changes in cerebellar and extracerebellar circuit
472 development, differences in the timing of PC perturbation could engage distinct
473 developmental processes (38). Our experiments were not designed to define discrete critical
474 periods for individual behavioral phenotypes. Nevertheless, the patterns observed across
475 intervention periods suggest that the long-term consequences of cerebellar perturbation
476 cannot be explained by duration of inhibition alone.

Several limitations should be considered. We were unable to assess behavior during acute PC inhibition because pilot CNO administration produced marked locomotor impairment (data not shown), and we therefore focused on long-term behavioral consequences. In addition, because we relied on a breeding-based strategy for DREADD expression, PC inhibition occurred broadly across the cerebellum. Previous studies using regionally targeted viral delivery have linked specific cerebellar lobules to distinct behavioral phenotypes (26, 30, 71), whereas our approach did not permit comparable spatial resolution. Cre-independent expression from the hM4Di reporter allele was also observed outside the cerebellum, as previously reported (33). Although Cre-negative controls received the same CNO treatment, effects on Cre-independent hM4Di expression could have contributed to variability in baseline behavior. Finally, the transcriptomic analysis was exploratory and based on a limited number of biological replicates. The candidate transcriptional changes, particularly the apparent sex-dependent patterns, therefore require independent validation.

Cell-type-resolved transcriptomic approaches will be important for identifying the cellular substrates underlying the observed molecular responses and determining whether sex-dependent transcriptional changes arise within the cerebellum itself, in downstream circuits, or both. Defining the mechanisms underlying male-biased behavioral susceptibility,

494 including the respective contributions of sex chromosomes, sex steroids, and sex-dependent
495 cerebellar maturation, will also be important. Finally, sex-stratified longitudinal studies of
496 individuals with perinatal cerebellar injury could test whether comparable early cerebellar
497 insults produce different developmental outcomes in males and females, including both core
498 and associated features of ASD.

499 In conclusion, transient developmental perturbation of Purkinje cell function during
500 the early postnatal period produced modest behavioral alterations relevant to ASD in
501 adulthood, with a pronounced male bias. The resulting phenotypes encompassed both core
502 ASD-like behaviors and associated features of ASD, including motor, sensory, and sleep-
503 related abnormalities. Accompanying forebrain transcriptional changes further suggest that
504 early cerebellar dysfunction can exert long-range influences on distant brain regions,
505 potentially through a developmental diaschisis-like mechanism. Together, these findings
506 support developmental cerebellar dysfunction as a potential shared substrate linking diverse
507 core and associated ASD-relevant phenotypes. Furthermore, sex-dependent vulnerability to
508 developmental cerebellar dysfunction may contribute to the male-biased prevalence of ASD
509 in humans, providing new insight into its pathogenesis.
510

Compliance with ethical standards

Conflict of interest

The authors declare that they have no conflict of interest.

Acknowledgements

We thank Dr. Mitsuhiko Yamada for his continuous support of our work. We also thank Mai Tamaki and Hiromi Muramatsu for their administrative assistance and all members of our laboratory for their support. This research was supported by Japan Society for the Promotion of Science KAKENHI Grant-in-Aid for Research Activity Start-up (Grant Number JP21K20705 to SK), Japan Foundation of Institute for Neurology and Psychiatry Research Grant for Young Researchers (to SK), Meiji Yasuda Mental Health Foundation (to SK), The Mother and Child Health Foundation (to SK), and Intramural Research Grant (3-1 and 6-1) for Neurological and Psychiatric Disorders provided by the National Center of Neurology and Psychiatry, Japan (to HM). We thank the staff of the Laboratory Animal Center at National Center of Neurology and Psychiatry for their expert animal care and support.

Author contributions

S.K. and H.M. conceptualized the study. S.K. performed most experiments. H.M. performed electrophysiological recording. S.K. wrote the manuscript under the supervision of H.M. and K.I.

References

1. Zablotsky B, Black LI, Maenner MJ, Schieve LA, Blumberg SJ. Estimated Prevalence of Autism and Other Developmental Disabilities Following Questionnaire Changes in the 2014 National Health Interview Survey. Natl Health Stat Report. 2015(87):1-20.
2. Saito M, Hirota T, Sakamoto Y, Adachi M, Takahashi M, Osato-Kaneda A, et al. Prevalence and cumulative incidence of autism spectrum disorders and the patterns of co-occurring neurodevelopmental disorders in a total population sample of 5-year-old children. Mol Autism. 2020;11(1):35.
3. Bourgeron T. Current knowledge on the genetics of autism and propositions for future research. C R Biol. 2016;339(7-8):300-7.
4. Shaw KA, Williams S, Patrick ME, Valencia-Prado M, Durkin MS, Howerton EM, et al. Prevalence and Early Identification of Autism Spectrum Disorder Among Children Aged 4 and 8 Years - Autism and Developmental Disabilities Monitoring Network, 16 Sites, United States, 2022. MMWR Surveill Summ. 2025;74(2):1-22.
5. Fombonne E. Epidemiology of pervasive developmental disorders. Pediatr Res. 2009;65(6):591-8.
6. Zoghbi HY, Bear MF. Synaptic dysfunction in neurodevelopmental disorders associated with autism and intellectual disabilities. Cold Spring Harb Perspect Biol. 2012;4(3).
7. Estes ML, McAllister AK. Maternal immune activation: Implications for neuropsychiatric disorders. Science. 2016;353(6301):772-7.
8. Takumi T, Tamada K, Hatanaka F, Nakai N, Bolton PF. Behavioral neuroscience of autism. Neurosci Biobehav Rev. 2020;110:60-76.
9. Tseng CJ, McDougle CJ, Hooker JM, Zürcher NR. Epigenetics of Autism Spectrum Disorder: Histone Deacetylases. Biol Psychiatry. 2022;91(11):922-33.
10. Willsey HR, Willsey AJ, Wang B, State MW. Genomics, convergent neuroscience and progress in understanding autism spectrum disorder. Nat Rev Neurosci. 2022;23(6):323-41.

11. Geschwind DH, State MW. Gene hunting in autism spectrum disorder: on the path to precision medicine. Lancet Neurol. 2015;14(11):1109-20.
12. Kamijo S, Miwa H, Ikeda K. Autism Spectrum Disorder: Integrating Genetic and Environmental Risk. Cells. 2026;15(11).
13. Wang SS, Kloth AD, Badura A. The cerebellum, sensitive periods, and autism. Neuron. 2014;83(3):518-32.
14. Mosconi MW, Wang Z, Schmitt LM, Tsai P, Sweeney JA. The role of cerebellar circuitry alterations in the pathophysiology of autism spectrum disorders. Front Neurosci. 2015;9:296.
15. Schmahmann JD, Guell X, Stoodley CJ, Halko MA. The Theory and Neuroscience of Cerebellar Cognition. Annu Rev Neurosci. 2019;42:337-64.
16. Stoodley CJ, Limperopoulos C. Structure-function relationships in the developing cerebellum: Evidence from early-life cerebellar injury and neurodevelopmental disorders. Semin Fetal Neonatal Med. 2016;21(5):356-64.
17. Limperopoulos C, Bassan H, Gauvreau K, Robertson RL, Jr., Sullivan NR, Benson CB, et al. Does cerebellar injury in premature infants contribute to the high prevalence of long-term cognitive, learning, and behavioral disability in survivors? Pediatrics. 2007;120(3):584-93.
18. Fatemi SH, Aldinger KA, Ashwood P, Bauman ML, Blaha CD, Blatt GJ, et al. Consensus paper: pathological role of the cerebellum in autism. Cerebellum. 2012;11(3):777-807.
19. D'Mello AM, Crocetti D, Mostofsky SH, Stoodley CJ. Cerebellar gray matter and lobular volumes correlate with core autism symptoms. Neuroimage Clin. 2015;7:631-9.
20. Cupolillo D, Hoxha E, Faralli A, De Luca A, Rossi F, Tempia F, et al. Autistic-Like Traits and Cerebellar Dysfunction in Purkinje Cell PTEN Knock-Out Mice. Neuropsychopharmacology. 2016;41(6):1457-66.
21. Gibson JM, Howland CP, Ren C, Howland C, Vernino A, Tsai PT. A Critical Period for Development of Cerebellar-Mediated Autism-Relevant Social Behavior. J Neurosci. 2022;42(13):2804-23.
22. Gibson JM, Vazquez AH, Yamashiro K, Jakkamsetti V, Ren C, Lei K, et

al. Cerebellar contribution to autism-relevant behaviors in fragile X syndrome models. Cell Rep. 2023;42(12):113533.
23. Kelly E, Meng F, Fujita H, Morgado F, Kazemi Y, Rice LC, et al. Regulation of autism-relevant behaviors by cerebellar-prefrontal cortical circuits. Nat Neurosci. 2020;23(9):1102-10.
24. Peter S, Ten Brinke MM, Stedehouder J, Reinelt CM, Wu B, Zhou H, et al. Dysfunctional cerebellar Purkinje cells contribute to autism-like behaviour in Shank2-deficient mice. Nat Commun. 2016;7:12627.
25. Reith RM, McKenna J, Wu H, Hashmi SS, Cho SH, Dash PK, et al. Loss of Tsc2 in Purkinje cells is associated with autistic-like behavior in a mouse model of tuberous sclerosis complex. Neurobiol Dis. 2013;51:93-103.
26. Stoodley CJ, D'Mello AM, Ellegood J, Jakkamsetti V, Liu P, Nebel MB, et al. Altered cerebellar connectivity in autism and cerebellar-mediated rescue of autism-related behaviors in mice. Nat Neurosci. 2017;20(12):1744-51.
27. Yamashiro K, Hori K, Lai ESK, Aoki R, Shimaoka K, Arimura N, et al. AUTS2 Governs Cerebellar Development, Purkinje Cell Maturation, Motor Function and Social Communication. iScience. 2020;23(12):101820.
28. Tsai PT, Hull C, Chu Y, Greene-Colozzi E, Sadowski AR, Leech JM, et al. Autistic-like behaviour and cerebellar dysfunction in Purkinje cell Tsc1 mutant mice. Nature. 2012;488(7413):647-51.
29. Tsai PT, Rudolph S, Guo C, Ellegood J, Gibson JM, Schaeffer SM, et al. Sensitive Periods for Cerebellar-Mediated Autistic-like Behaviors. Cell Rep. 2018;25(2):357-67.e4.
30. Badura A, Verpeut JL, Metzger JW, Pereira TD, Pisano TJ, Deverett B, et al. Normal cognitive and social development require posterior cerebellar activity. Elife. 2018;7.e36401.
31. Micai M, Fatta LM, Gila L, Caruso A, Salvitti T, Fulceri F, et al. Prevalence of co-occurring conditions in children and adults with autism spectrum disorder: A systematic review and meta-analysis. Neurosci Biobehav Rev. 2023;155:105436.

32. Barski JJ, Dethleffsen K, Meyer M. Cre recombinase expression in cerebellar Purkinje cells. Genesis. 2000;28(3-4):93-8.
33. Zhu H, Aryal DK, Olsen RH, Urban DJ, Swearingen A, Forbes S, et al. Cre-dependent DREADD (Designer Receptors Exclusively Activated by Designer Drugs) mice. Genesis. 2016;54(8):439-46.
34. Schalbetter SM, Mueller FS, Scarborough J, Richetto J, Weber-Stadlbauer U, Meyer U, et al. Oral application of clozapine-N-oxide using the micropipette-guided drug administration (MDA) method in mouse DREADD systems. Lab Anim (NY). 2021;50(3):69-75.
35. Fujihara K, Miwa H, Kakizaki T, Kaneko R, Mikuni M, Tanahira C, et al. Glutamate Decarboxylase 67 Deficiency in a Subset of GABAergic Neurons Induces Schizophrenia-Related Phenotypes. Neuropsychopharmacology. 2015;40(10):2475-86.
36. Chen L, McKenna JT, Leonard MZ, Yanagawa Y, McCarley RW, Brown RE. GAD67-GFP knock-in mice have normal sleep-wake patterns and sleep homeostasis. Neuroreport. 2010;21(3):216-20.
37. Roth BL. DREADDs for Neuroscientists. Neuron. 2016;89(4):683-94.
38. van der Heijden ME, Gill JS, Sillitoe RV. Abnormal Cerebellar Development in Autism Spectrum Disorders. Dev Neurosci. 2021;43(3-4):181-90.
39. van der Heijden ME, Sillitoe RV. Interactions Between Purkinje Cells and Granule Cells Coordinate the Development of Functional Cerebellar Circuits. Neuroscience. 2021;462:4-21.
40. Fiorenza MT, La Rosa P, Canterini S, Erickson RP. The Cerebellum in Niemann-Pick C1 Disease: Mouse Versus Man. Cerebellum. 2023;22(1):102-19.
41. Yang M, Silverman JL, Crawley JN. Automated three-chambered social approach task for mice. Curr Protoc Neurosci. 2011;Chapter 8:Unit 8.26.
42. Rein B, Ma K, Yan Z. A standardized social preference protocol for measuring social deficits in mouse models of autism. Nat Protoc. 2020;15(10):3464-77.
43. Nakatani J, Tamada K, Hatanaka F, Ise S, Ohta H, Inoue K, et al. Abnormal behavior in a chromosome-engineered mouse model for

human 15q11-13 duplication seen in autism. Cell. 2009;137(7):1235-46.
44. Gawel K, Gibula E, Marszalek-Grabska M, Filarowska J, Kotlinska JH. Assessment of spatial learning and memory in the Barnes maze task in rodents-methodological consideration. Naunyn Schmiedebergs Arch Pharmacol. 2019;392(1):1-18.
45. Tang S, Terzic B, Wang IJ, Sarmiento N, Sizov K, Cui Y, et al. Altered NMDAR signaling underlies autistic-like features in mouse models of CDKL5 deficiency disorder. Nat Commun. 2019;10(1):2655.
46. Miller HL, Sherrod GM, Mauk JE, Fears NE, Hynan LS, Tamplain PM. Shared Features or Co-occurrence? Evaluating Symptoms of Developmental Coordination Disorder in Children and Adolescents with Autism Spectrum Disorder. J Autism Dev Disord. 2021;51(10):3443-55.
47. Tomchek SD, Dunn W. Sensory processing in children with and without autism: a comparative study using the short sensory profile. Am J Occup Ther. 2007;61(2):190-200.
48. Robertson CE, Baron-Cohen S. Sensory perception in autism. Nat Rev Neurosci. 2017;18(11):671-84.
49. Cohen S, Conduit R, Lockley SW, Rajaratnam SM, Cornish KM. The relationship between sleep and behavior in autism spectrum disorder (ASD): a review. J Neurodev Disord. 2014;6(1):44.
50. Cheng CH, Chan PS, Hsu SC, Liu CY. Meta-analysis of sensorimotor gating in patients with autism spectrum disorders. Psychiatry Res. 2018;262:413-9.
51. Chen H, Yang T, Chen J, Chen L, Dai Y, Zhang J, et al. Sleep problems in children with autism spectrum disorder: a multicenter survey. BMC Psychiatry. 2021;21(1):406.
52. Zwicker JG, Missiuna C, Harris SR, Boyd LA. Developmental coordination disorder: a review and update. Eur J Paediatr Neurol. 2012;16(6):573-81.
53. Mannion A, Leader G. Sleep Problems in Autism Spectrum Disorder: A Literature Review. Review Journal of Autism and Developmental Disorders. 2014;1(2):101-9.
54. Galli J, Loi E, Visconti LM, Mattei P, Eusebi A, Calza S, et al. Sleep

Disturbances in Children Affected by Autism Spectrum Disorder. Front Psychiatry. 2022;13:736696.
55. Roux S, Lohof A, Ben-Ari Y, Poulain B, Bossu JL. Maturation of GABAergic Transmission in Cerebellar Purkinje Cells Is Sex Dependent and Altered in the Valproate Model of Autism. Front Cell Neurosci. 2018;12:232.
56. Roux S, Bailly Y, Bossu JL. Regional and sex-dependent alterations in Purkinje cell density in the valproate mouse model of autism. Neuroreport. 2019;30(2):82-8.
57. Wang R, Tan J, Guo J, Zheng Y, Han Q, So KF, et al. Aberrant Development and Synaptic Transmission of Cerebellar Cortex in a VPA Induced Mouse Autism Model. Front Cell Neurosci. 2018;12:500.
58. Hadj-Sahraoui N, Frédéric F, Delhaye-Bouchaud N, Mariani J. Gender effect on Purkinje cell loss in the cerebellum of the heterozygous reeler mouse. J Neurogenet. 1996;11(1-2):45-58.
59. Abel JM, Witt DM, Rissman EF. Sex differences in the cerebellum and frontal cortex: roles of estrogen receptor alpha and sex chromosome genes. Neuroendocrinology. 2011;93(4):230-40.
60. Dean SL, Knutson JF, Krebs-Kraft DL, McCarthy MM. Prostaglandin E2 is an endogenous modulator of cerebellar development and complex behavior during a sensitive postnatal period. Eur J Neurosci. 2012;35(8):1218-29.
61. Xu FX, Wang XT, Cai XY, Liu JY, Guo JW, Yang F, et al. Purkinje-cell-specific MeCP2 deficiency leads to motor deficits and autistic-like behavior due to aberrations in PTP1B-TrkB-SK signaling. Cell Rep. 2023;42(12):113559.
62. Yang X, Yin H, Wang X, Sun Y, Bian X, Zhang G, et al. Social Deficits and Cerebellar Degeneration in Purkinje Cell Scn8a Knockout Mice. Front Mol Neurosci. 2022;15:822129.
63. Locke TM, Fujita H, Hunker A, Johanson SS, Darvas M, du Lac S, et al. Purkinje Cell-Specific Knockout of Tyrosine Hydroxylase Impairs Cognitive Behaviors. Front Cell Neurosci. 2020;14:228.
64. Oostland M, Buijink MR, van Hooft JA. Serotonergic control of Purkinje

cell maturation and climbing fibre elimination by 5-HT3 receptors in the juvenile mouse cerebellum. J Physiol. 2013;591(7):1793-807.
65. Ingram JL, Peckham SM, Tisdale B, Rodier PM. Prenatal exposure of rats to valproic acid reproduces the cerebellar anomalies associated with autism. Neurotoxicol Teratol. 2000;22(3):319-24.
66. Vacher CM, Lacaille H, O'Reilly JJ, Salzbank J, Bakalar D, Sebaoui S, et al. Placental endocrine function shapes cerebellar development and social behavior. Nat Neurosci. 2021;24(10):1392-401.
67. Kozareva V, Martin C, Osorno T, Rudolph S, Guo C, Vanderburg C, et al. A transcriptomic atlas of mouse cerebellar cortex comprehensively defines cell types. Nature. 2021;598(7879):214-9.
68. Takayama C, Inoue Y. Transient expression of GABAA receptor alpha2 and alpha3 subunits in differentiating cerebellar neurons. Brain Res Dev Brain Res. 2004;148(2):169-77.
69. Newhart A, Powers SL, Shastrula PK, Sierra I, Joo LM, Hayden JE, et al. RNase P protein subunit Rpp29 represses histone H3.3 nucleosome deposition. Mol Biol Cell. 2016;27(7):1154-69.
70. Funk OH, Qalieh Y, Doyle DZ, Lam MM, Kwan KY. Postmitotic accumulation of histone variant H3.3 in new cortical neurons establishes neuronal chromatin, transcriptome, and identity. Proc Natl Acad Sci U S A. 2022;119(32):e2116956119.
71. Verpeut JL, Bergeler S, Kislin M, William Townes F, Klibaite U, Dhanerawala ZM, et al. Cerebellar contributions to a brainwide network for flexible behavior in mice. Commun Biol. 2023;6(1):605.

Figure legends

Fig. 1 Establishment and validation of a temporally controlled chemogenetic Purkinje cell inhibition paradigm during early postnatal development. A Breeding strategy and experimental timeline for transient developmental Purkinje cell inhibition. Heterozygous *L7*-

Cre mice were crossed with homozygous *LSL-hM4Di-mCitrine* mice to enable Cre-dependent expression of inhibitory DREADD (hM4Di) and mCitrine in Purkinje cells. Clozapine-N-oxide (CNO) was administered orally during development. Three inhibition windows were tested: P11–15, P11–20, and P21–30. Mice were subsequently allowed to mature, and behavioral and other analyses were performed from ≥8 weeks of age. **B** Cre-dependent expression of mCitrine in Purkinje cells at P16. Representative cerebella from Cre-negative (top) and Cre-positive (bottom) mice are shown. Scale bars, 200 μm. **C–E** Effects of CNO on Purkinje cell-mediated IPSCs in DCN neurons. **C** Schematic diagram of the electrophysiological recording setup (top). Representative IPSC traces before (1) and after application of 10 μM CNO (2), as indicated in the time course plots in **D** and **E** (bottom). **D** Time course of normalized evoked IPSC amplitudes and paired comparison between baseline and CNO conditions (left). IPSC amplitudes during CNO application were 79 ± 8% of baseline (right, $P = 0.0354$, two-tailed paired *t*-test, N = 8, mean ± SEM). **E** Time course of the paired-pulse ratio (PPR) (left). The mean change in PPR was 0.22 ± 0.08 (right, $P = 0.0233$, two-tailed paired *t*-test, N = 8, mean ± SEM). **F** Adult Purkinje cell density after developmental inhibition. Linear Purkinje cell density (cells/mm) in lobule IX in adults following PC inhibition during P11–15, P11–20, or P21–30 and their respective controls.

775 Left, males; right, females. Data are shown as medians with individual data points. Statistical
776 comparisons were performed using two-tailed unpaired *t*-tests. Sample sizes and *P* values are
777 indicated: males—P11–15 (control vs inhibited: $N = 12, 11$; $P = 0.2066$), P11–20 ($N = 16,$
778 14; $P = 0.2137$), P21–30 ($N = 13, 9$; $P = 0.9004$); females—P11–15 ($N = 13, 11$; $P = 0.3891$),
779 P11–20 ($N = 14, 14$; $P = 0.8837$), P21–30 ($N = 10, 8$; $P = 0.4620$).
780
781 **Fig. 2 Social preference and grooming behavior following developmental Purkinje cell**
782 **inhibition. A** Social preference index in the three-chamber social interaction test (preference
783 for the social stimulus over the object stimulus; see Materials and Methods for calculation).
784 Data are shown separately by sex (left, males; right, females) across three inhibition windows
785 (P11–15, P11–20, P21–30). Male: P11–15 control vs PC-inhibited (N = 17, 20; $P = 0.0417$);
786 P11–20 (N = 25, 20; $P = 0.4617$); P21–30 (N = 13, 13; $P = 0.5788$). Female: P11–15 (N =
787 18, 18; $P = 0.9875$); P11–20 (N = 28, 26; $P = 0.2896$); P21–30 (N = 12, 11; $P = 0.4134$). **B**
788 Total grooming time during a 10-min grooming session, shown separately by sex across
789 inhibition windows. Male: P11–15 control vs PC-inhibited (N = 16, 16; $P = 0.8672$); P11–
790 20 (N = 25, 20; $P = 0.1117$); P21–30 (N = 13, 13; $P = 0.0568$). Female: P11–15 (N = 16, 14;
791 $P = 0.4726$); P11–20 (N = 28, 25; $P = 0.9760$); P21–30 (N = 12, 11; $P = 0.8660$). Data are

792 presented as medians with individual data points. Statistical comparisons were performed
793 using two-tailed Mann–Whitney *U* tests.
794
795 **Fig. 3 Developmental Purkinje cell inhibition does not impair spatial learning/memory**
796 **but alters cognitive flexibility in the reversal Barnes maze. A** Reversal Barnes maze
797 paradigm and arena schematic. Adult mice that received developmental PC inhibition (CNO
798 administration during P11–20 or P21–30) underwent training (days 1-5), a probe test (day 6),
799 reversal training (days 7-9) and reversal probe test (day 10). The escape-hole position was
800 switched on day 7. Right, definition of quadrants and relative positions of the original ("old")
801 and switched ("new") goal locations. **B** Primary latency to reach the escape hole during
802 training and reversal training. Left, males; right, females. Data are shown as mean ± SEM.
803 Two-way repeated-measures ANOVA was used. Male: P11–20 (N = 17, 11; genotype effect,
804 $P = 0.9556$; reversal training genotype effect, $P = 0.8424$); P21–30 (N = 13, 13; genotype
805 effect, $P = 0.9407$; reversal training genotype effect, $P = 0.8765$). Female: P11–20 (N = 18,
806 14; genotype effect, $P = 0.5588$; reversal training genotype effect, $P = 0.2196$); P21–30 (N =
807 12, 11; genotype effect, $P = 0.1696$; reversal training genotype effect, $P = 0.5891$). **C**
808 Quadrant investigation time during the probe and reversal probe tests. Bars represent time

spent exploring each quadrant (west/target/east/opposite). For each phase, the "target" quadrant corresponds to the goal location for that phase (original target during the probe test; new target during the reversal probe test; see schematic in **A**). Panels are shown for P11–20 (top) and P21–30 (bottom), separated by sex (left, male; right, female). Data are shown as mean ± SEM.

Fig. 4 Developmental Purkinje cell inhibition produces timing- and sex-dependent changes in fine motor coordination and auditory sensorimotor processing. A Adult mice (≥8 weeks) were tested on an accelerating rotarod to assess motor coordination and motor skill learning. Plots show latency to fall across six consecutive trials (mean ± SEM) for control (Cre-negative) and PC-inhibited (Cre-positive; hM4Di-expressing) mice that received CNO during the indicated developmental windows (P11–15, P11–20, or P21–30). Male (left): P11–15, N = 16 vs 16, genotype effect $P = 0.0404$; P11–20, N = 25 vs 18, $P = 0.2569$; P21–30, N = 13 vs 13, $P = 0.2694$. Female (right): P11–15, N = 16 vs 14, $P = 0.0912$; P11–20, N = 28 vs 26, $P = 0.3948$; P21–30, N = 12 vs 11, $P = 0.9529$. Statistical comparisons were performed using two-way repeated-measures ANOVA (genotype effect shown). **B** Acoustic startle responses at 110 and 120 dB. Left: male; P11–15 control vs PC-inhibited (N

826 = 14, 16; genotype effect, P = 0.0799); P11–20 (N = 24, 19; genotype effect, P = 0.4494);
827 P21–30 (N = 13, 12; genotype effect, P = 0.0620). Right: female; P11–15 (N = 15, 13;
828 genotype effect, P = 0.7336); P11–20 (N = 25, 23; genotype effect, P = 0.0649); P21–30 (N
829 = 11, 10; genotype effect, P = 0.1673). **C** Prepulse inhibition (PPI) in the same cohorts. Left:
830 male; P11–15 control vs PC-inhibited (N = 14, 16; genotype effect, P = 0.2288); P11–20 (N
831 = 24, 19; genotype effect, P = 0.0462); P21–30 (N = 13, 12; genotype effect, P = 0.0653).
832 Right: female; P11–15 (N = 15, 13; genotype effect, P = 0.0794); P11–20 (N = 25, 23;
833 genotype effect, P = 0.0097); P21–30 (N = 11, 10; genotype effect, P = 0.3889). Data are
834 shown as mean ± SEM. Two-way repeated-measures ANOVA was used for statistical
835 analysis.
836
837 **Fig. 5 Developmental perturbation of Purkinje cell function alters sleep–wake**
838 **architecture in male mice. A**, Representative 24-h hypnograms from adult male and female
839 PC-inhibited mice and controls following P11–20 inhibition. Gray shading indicates the dark
840 phase. W: wakefulness, NR: NREM sleep, R: REM sleep. **B**, Percentage of time spent in
841 wakefulness, NREM sleep, and REM sleep across the 24-h recording period, analyzed in 1-
842 h bins. **C**, Total time spent in wakefulness (top), NREM sleep (middle), and REM sleep

(bottom) over 24 h. Statistical analysis was performed using one-way ANOVA followed by Tukey's multiple comparisons test. One-way ANOVA: Wake, $F(3, 19) = 7.945$, $P = 0.0012$; NREM, $F(3, 19) = 7.610$, $P = 0.0015$; REM, $F(3, 19) = 2.882$, $P = 0.0628$. Significant pairwise differences are indicated in the figure. **D,** Time spent in wakefulness (top), NREM sleep (middle), and REM sleep (bottom) during the dark and light phases. Statistical analysis was performed using two-way ANOVA followed by Tukey's multiple comparisons test. Two-way ANOVA: wakefulness, phase, $F(1, 38) = 231.1$, $P < 0.0001$; group, $F(3, 38) = 7.249$, $P = 0.0006$; interaction, $F(3, 38) = 2.725$, $P = 0.0576$; NREM sleep, phase, $F(1, 38) = 198.8$, $P < 0.0001$; group, $F(3, 38) = 7.244$, $P = 0.0006$; interaction, $F(3, 38) = 2.612$, $P = 0.0654$; REM sleep, phase, $F(1, 38) = 195.1$, $P < 0.0001$; group, $F(3, 38) = 2.482$, $P = 0.0756$; interaction, $F(3, 38) = 1.645$, $P = 0.1951$. Significant pairwise differences are indicated in the figure. **E,** Number (upper) and mean duration (bottom) of wake (left), NREM (middle), and REM (right) episodes during the dark phase. Statistical analysis was performed using one-way ANOVA followed by Tukey's multiple comparisons test. One-way ANOVA: episode number, wakefulness, $F(3, 19) = 1.415$, $P = 0.2694$; NREM sleep, $F(3, 19) = 1.610$, $P = 0.2201$; REM sleep, $F(3, 19) = 3.006$, $P = 0.0559$; mean episode duration, wakefulness, $F(3, 19) = 1.547$, $P = 0.2349$; NREM sleep, $F(3, 19) = 0.4915$, $P = 0.6924$; REM sleep, $F(3, 19)$

860 = 0.2266, P = 0.8767. Significant pairwise differences are indicated in the figure. **F,**
861 Distribution of episode number (upper) and time contributed by episodes within each
862 duration range (bottom) during the dark phase. Episode durations were classified as <10, 10–
863 34, 34–130, 130–514, 514–1026, 1026–2048, 2048–4096, and >4096 s. Statistical analysis
864 was performed using two-way ANOVA followed by Tukey's multiple comparisons test.
865 Two-way ANOVA: episode number (top)—wakefulness, duration range, $F(7, 152) = 79.11$,
866 $P < 0.0001$; group, $F(3, 152) = 2.961$, $P = 0.0341$; interaction, $F(21, 152) = 1.166$, $P = 0.2887$;
867 NREM sleep, duration range, $F(4, 95) = 64.37$, $P < 0.0001$; group, $F(3, 95) = 3.346$, $P =$
868 0.0224; interaction, $F(12, 95) = 1.273$, $P = 0.2475$; REM sleep, duration range, $F(3, 76) =$
869 51.27, $P < 0.0001$; group, $F(3, 76) = 4.125$, $P = 0.0091$; interaction, $F(9, 76) = 0.9087$, $P =$
870 0.5223; time contribution (bottom)—wakefulness, duration range, $F(7, 152) = 60.13$, $P <$
871 0.0001; group, $F(3, 152) = 1.034$, $P = 0.3792$; interaction, $F(21, 152) = 4.558$, $P < 0.0001$;
872 NREM sleep, duration range, $F(4, 95) = 130.1$, $P < 0.0001$; group, $F(3, 95) = 7.791$, $P =$
873 0.0001; interaction, $F(12, 95) = 2.661$, $P = 0.0040$; REM sleep, duration range, $F(3, 76) =$
874 105.4, $P < 0.0001$; group, $F(3, 76) = 6.610$, $P = 0.0005$; interaction, $F(9, 76) = 2.074$, $P =$
875 0.0423. **G,** Number of transitions among vigilance states during the dark phase. Statistical
876 analysis was performed using two-way ANOVA followed by Tukey's multiple comparisons

877 test. Two-way ANOVA: transition type, F(4, 95) = 63.74, $P < 0.0001$; group, F(3, 95) =
878 4.966, $P = 0.0030$; interaction, F(12, 95) = 0.4186, $P = 0.9528$. W: wakefulness, NR: NREM
879 sleep, R: REM sleep. **H,** Mean normalized EEG power spectra during wakefulness, NREM
880 sleep, and REM sleep in the dark phase. Lines represent group-averaged EEG power spectra;
881 error bars are omitted for clarity. Data are presented as mean ± SEM. Male control, N = 6;
882 male PC-inhibited, N = 4; female control, N = 7; female PC-inhibited, N = 6. Data are
883 presented as mean ± SEM. P values are indicated as *$P < 0.05$, **$P < 0.01$, ***$P < 0.001$.
884 ****$P < 0.0001$.
885
886 **Fig. 6 Sex-dependent gene expression changes following developmental PC inhibition.**
887 **A** Experimental design for transcriptomic profiling. Male and female Cre-negative (control)
888 and Cre-positive (PC-inhibited; hM4Di-expressing) pups received oral CNO during P11–
889 15. Hindbrain and forebrain tissues were collected at P15 for bulk RNA sequencing and
890 subsequent validation. **B** RT–qPCR validation of candidate DEGs identified in males,
891 *Gabra2* and *Pop4* in hindbrain and forebrain. Panels (left to right): hindbrain *Pop4*,
892 forebrain *Pop4,* hindbrain *Gabra2,* forebrain *Gabra2.* Relative mRNA expression is shown
893 for controls and PC-inhibited mice of each sex (PC-inhibited values normalized to sex-

matched controls): *Pop4*—forebrain: male 131% [111–151%], female 107% [89–123%]; hindbrain: male 152% [143–168%], female 91% [68–112%]. *Gabra2*—forebrain: male 124% [111–137%], female 84% [74–106%]; hindbrain: male 115% [109–119%], female 89% [82–102%]. N = 3 mice per condition; individual data points are shown with horizontal bars indicating geometric means.

Tables

Table 1 Frequency of strategy switches in the reversal probe test

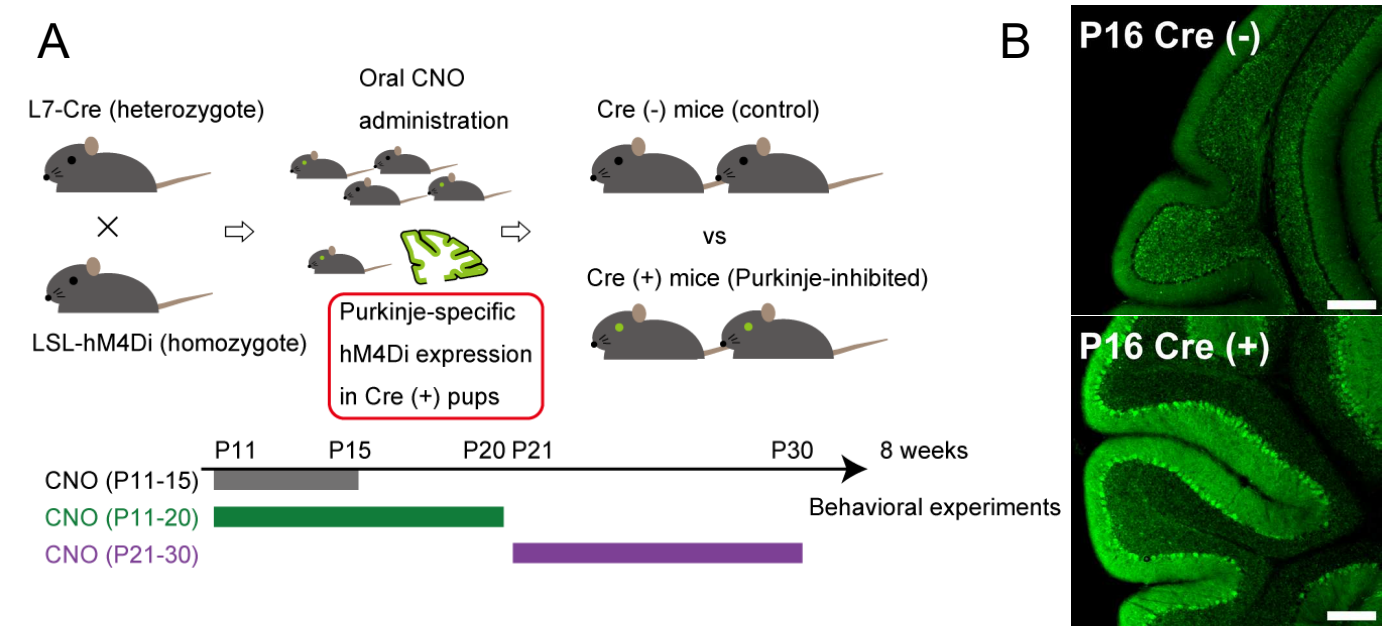
Sex and CNO treatment period	Control	PC-inhibited
Male (CNO P11-20)	53% (18/34)	23% (5/22)
Female (CNO P11-20)	47% (17/36)	46% (13/28)
Male (CNO P21-30)	35% (9/26)	42% (11/26)
Female (CNO P21-30)	29% (7/24)	36% (8/22)

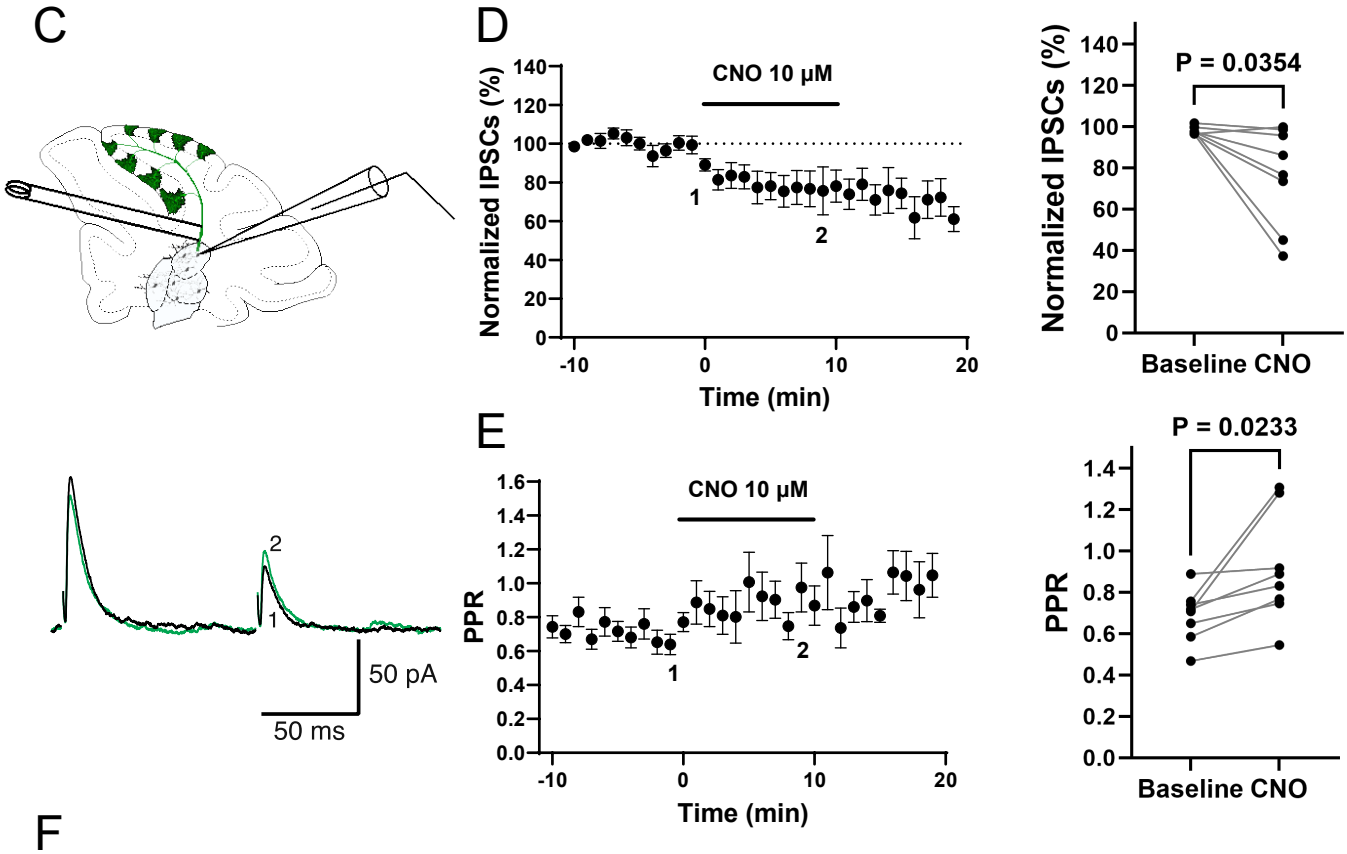
All mice received CNO during the indicated postnatal period.

The frequency of strategy switches was compared between PC-inhibited mice and controls. N values are shown as PC-inhibited mice, controls. Male: P11–20 (N = 17, 11; $P = 0.0298$); Female P11–20 (N = 18, 14; $P = 1.0000$). Male: P21–30 (N = 13, 13; $P = 0.7342$); Female P21–30 (N = 12, 11; $P = 0.7549$). Statistical comparisons were performed using Fisher's

907 exact tests.

Figure 1


A
L7-Cre (heterozygote)
LSL-hM4Di (homozygote)
Oral CNO administration
Purkinje-specific hM4Di expression in Cre (+) pups
Cre (-) mice (control)
vs
Cre (+) mice (Purkinje-inhibited)
P11
P15
P20 P21
P30
8 weeks
CNO (P11-15)
CNO (P11-20)
CNO (P21-30)
Behavioral experiments
B
P16 Cre (-)
P16 Cre (+)


C
D
CNO 10 μM
Normalized IPSCs (%)
Time (min)
P = 0.0354
Baseline CNO
E
CNO 10 μM
PPR
Time (min)
P = 0.0233
Baseline CNO
50 pA
50 ms

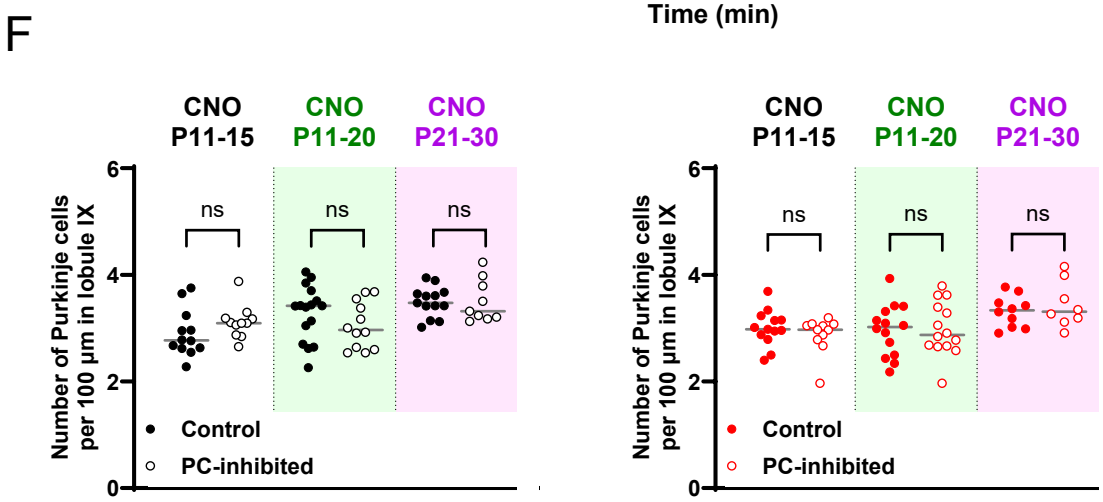

F
CNO P11-15
CNO P11-20
CNO P21-30
ns
Number of Purkinje cells per 100 μm in lobule IX
Control
PC-inhibited

Figure 2

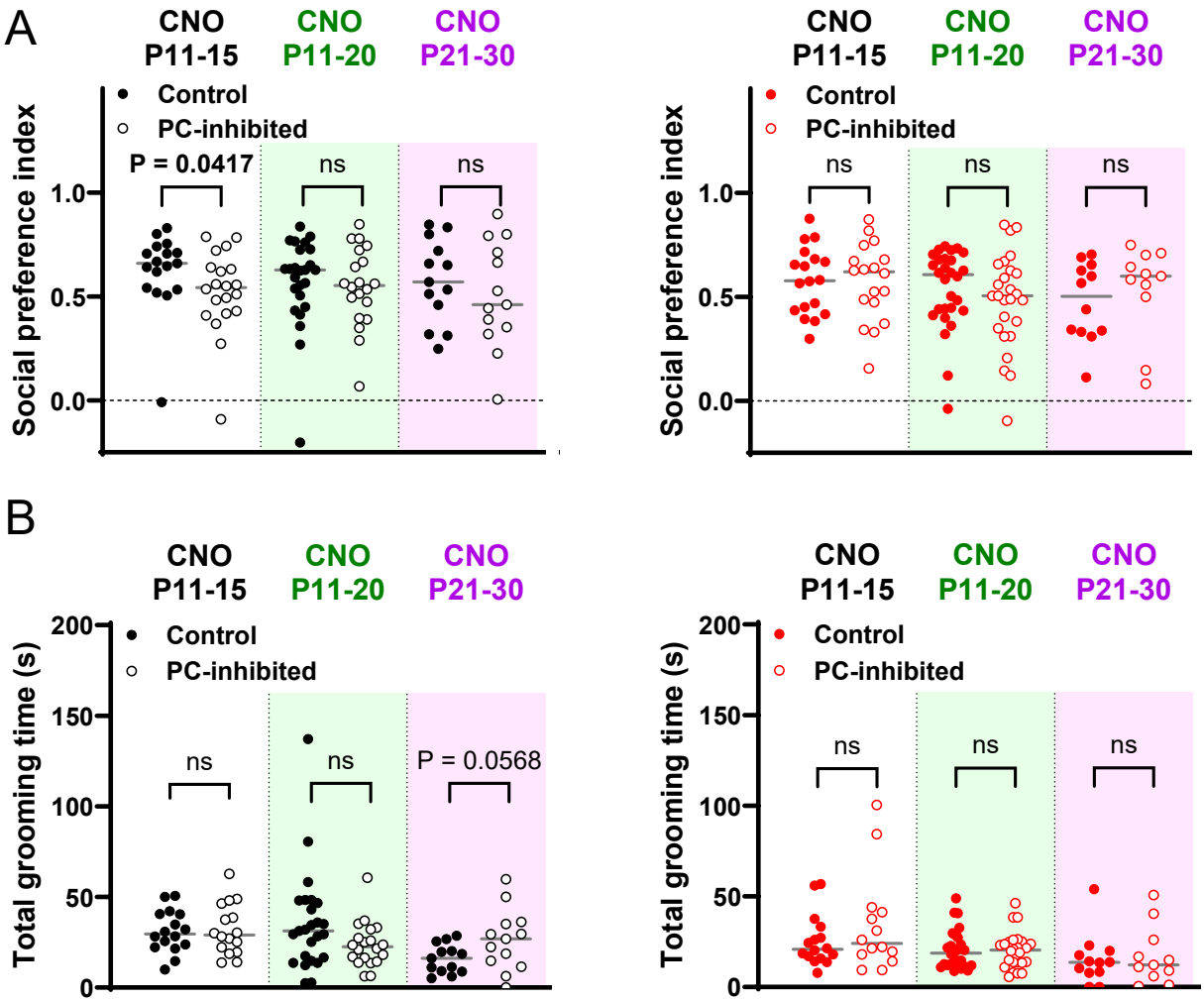
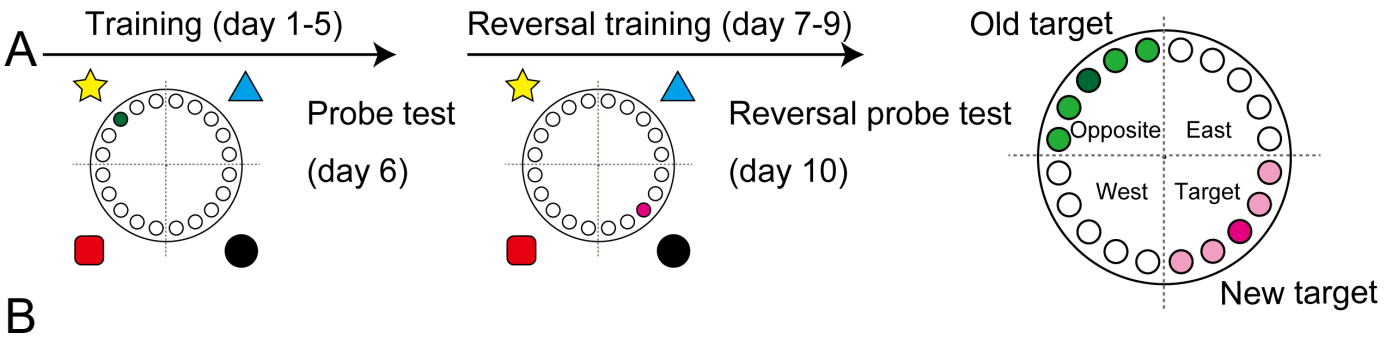
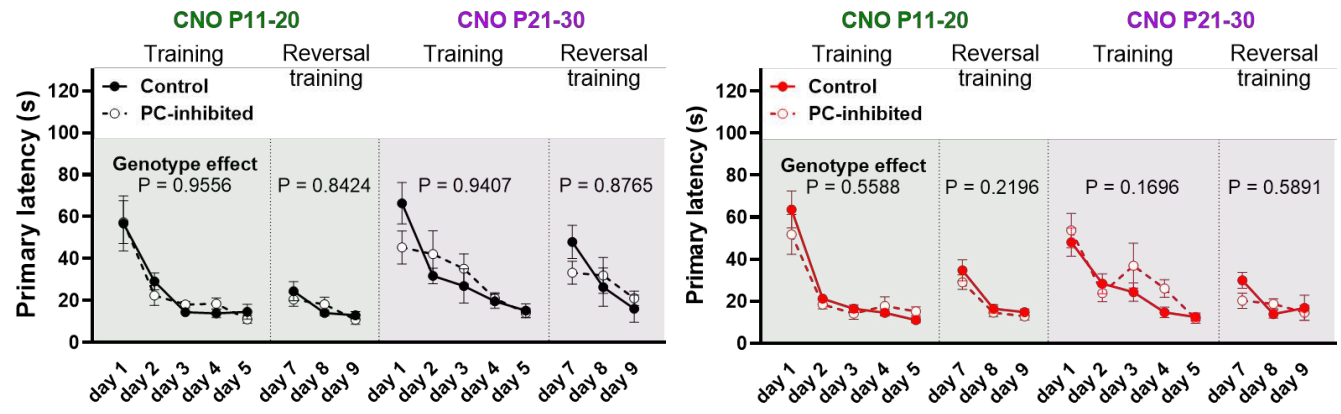

A
CNO P11-15
CNO P11-20
CNO P21-30
Control
PC-inhibited
P = 0.0417
ns
ns
Social preference index
1.0
0.5
0.0
ns
ns
ns
B
CNO P11-15
CNO P11-20
CNO P21-30
Control
PC-inhibited
Total grooming time (s)
200
150
100
50
0
ns
ns
P = 0.0568
ns
ns
ns

Figure 3


A
Training (day 1-5)
Probe test
(day 6)
Reversal training (day 7-9)
Reversal probe test
(day 10)
Old target
Opposite
East
West
Target
New target


B
CNO P11-20
CNO P21-30
Training
Reversal training
Control
PC-inhibited
Primary latency (s)
Genotype effect
P = 0.9556
P = 0.8424
P = 0.9407
P = 0.8765
P = 0.5588
P = 0.2196
P = 0.1696
P = 0.5891
day 1 day 2 day 3 day 4 day 5 day 7 day 8 day 9

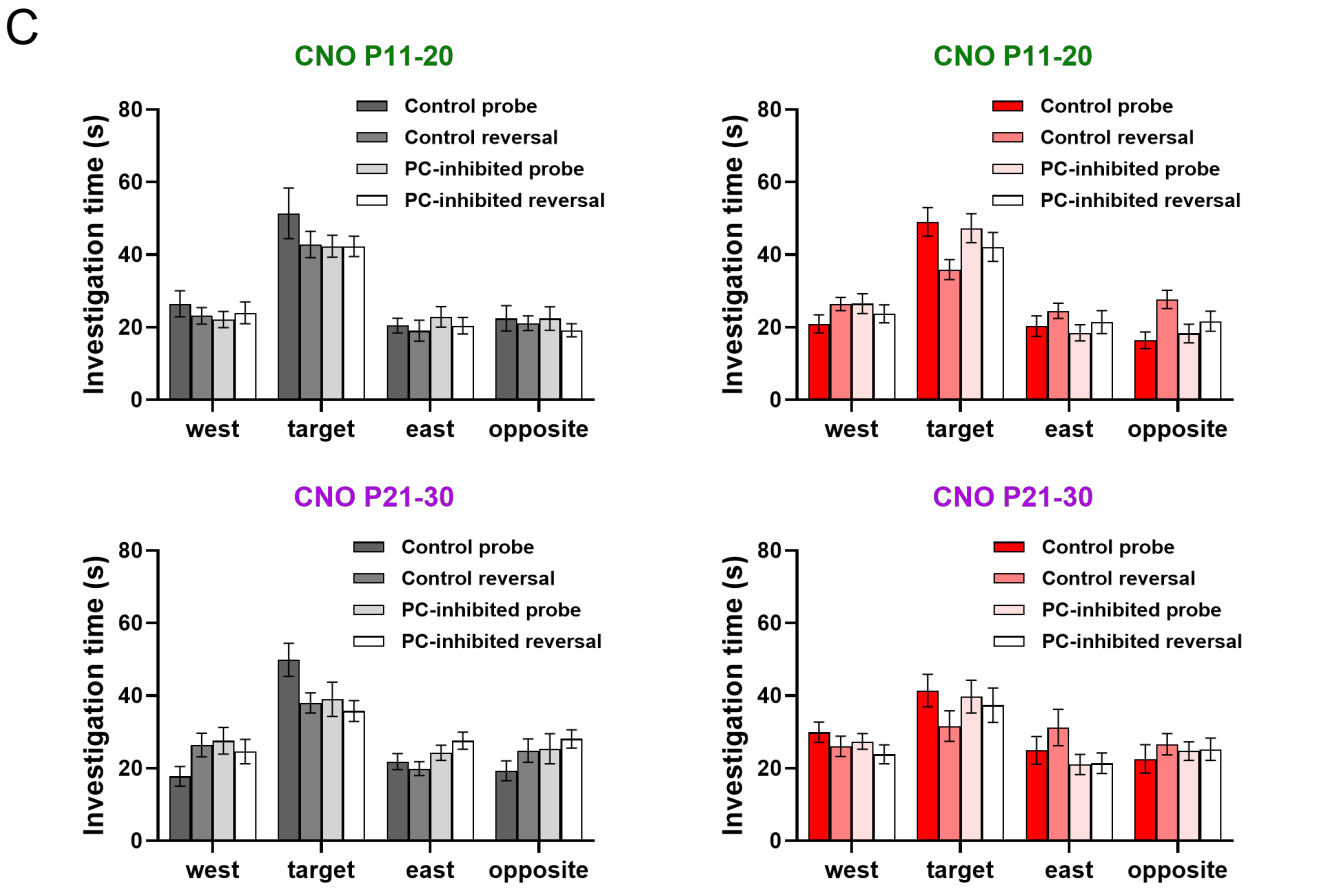

C
CNO P11-20
CNO P21-30
Control probe
Control reversal
PC-inhibited probe
PC-inhibited reversal
Investigation time (s)
west
target
east
opposite

Figure 4

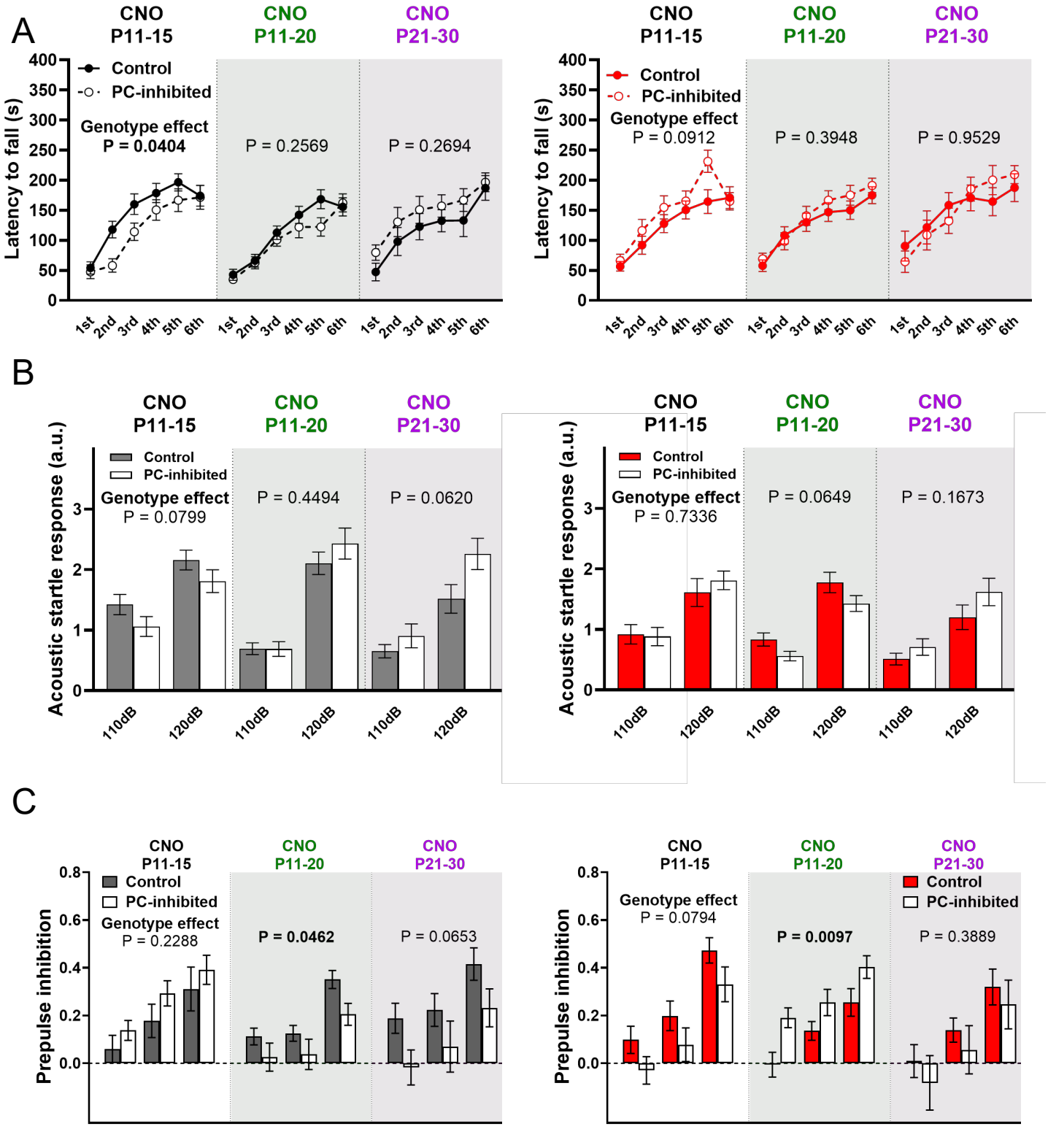

A
CNO P11-15
CNO P11-20
CNO P21-30
Control
PC-inhibited
Genotype effect
P = 0.0404
P = 0.2569
P = 0.2694
Latency to fall (s)
1st 2nd 3rd 4th 5th 6th
Genotype effect
P = 0.0912
P = 0.3948
P = 0.9529
B
Acoustic startle response (a.u.)
Genotype effect
P = 0.0799
P = 0.4494
P = 0.0620
Genotype effect
P = 0.7336
P = 0.0649
P = 0.1673
110dB 120dB
C
Prepulse inhibition
Genotype effect
P = 0.2288
P = 0.0462
P = 0.0653
Genotype effect
P = 0.0794
P = 0.0097
P = 0.3889

Figure 5

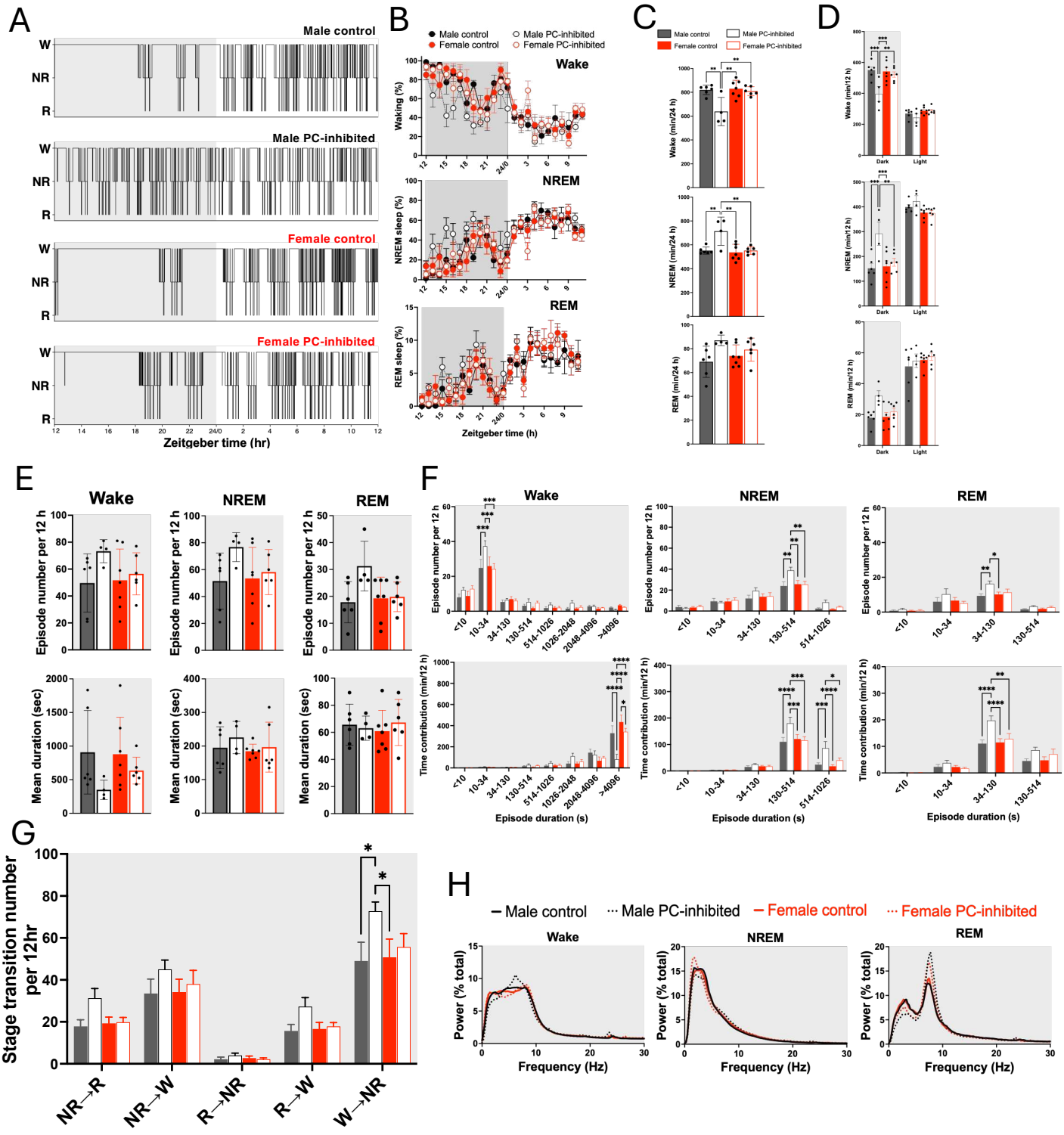
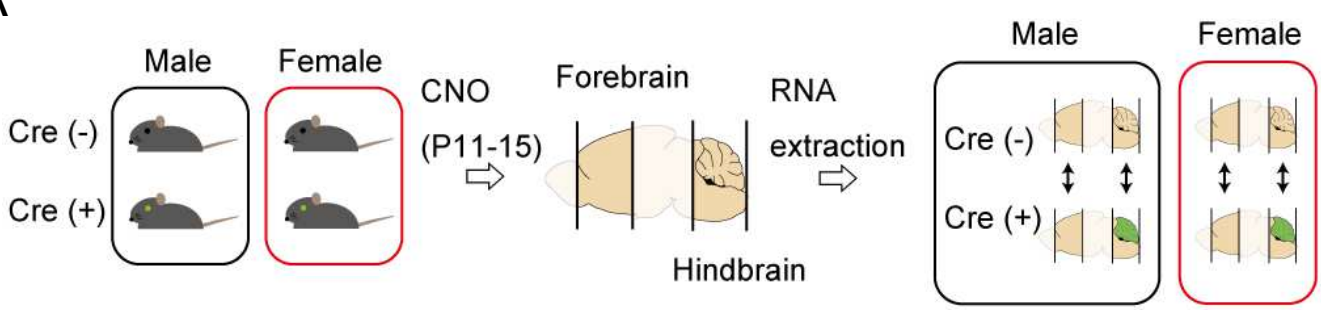
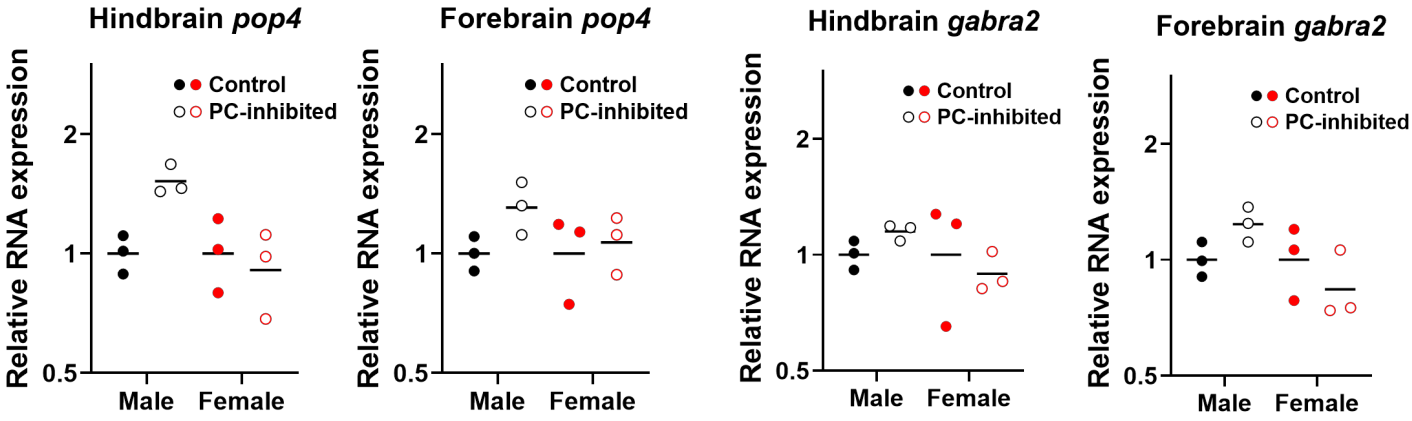

A
Male control
Male PC-inhibited
Female control
Female PC-inhibited
W
NR
R
Zeitgeber time (hr)
B
Male control
Female control
Male PC-inhibited
Female PC-inhibited
Wake
NREM
REM
Waking (%)
NREM sleep (%)
REM sleep (%)
Zeitgeber time (h)
C
Wake (min/24 h)
NREM (min/24 h)
REM (min/24 h)
D
Wake (min/12 h)
NREM (min/12 h)
REM (min/12 h)
Dark
Light
E
Wake
NREM
REM
Episode number per 12 h
Mean duration (sec)
F
Episode number per 12 h
Time contribution (min/12 h)
<10
10-34
34-130
130-514
514-1026
1026-2048
2048-4096
>4096
Episode duration (s)
G
Stage transition number per 12hr
NR→R
NR→W
R→NR
R→W
W→NR
H
Male control
Male PC-inhibited
Female control
Female PC-inhibited
Power (% total)
Frequency (Hz)

Figure 6

A


Male
Female
Cre (-)
Cre (+)
CNO
(P11-15)
Forebrain
Hindbrain
RNA
extraction
Male
Female
Cre (-)
Cre (+)

B


Hindbrain pop4
Forebrain pop4
Hindbrain gabra2
Forebrain gabra2
Relative RNA expression
Control
PC-inhibited
2
1
0.5
Male
Female

Supplementary Files

This is a list of supplementary files associated with this preprint. Click to download.

- KamijoetalASDSupplementMP.pdf